in the absence of a collision gas are not spontaneous (true metastables) but are also CID, caused by residual gas pressure in the 10^{-6} Torr range in the ion path. This residual pressure is due to the rather high pressure (0.2–0.5 Torr) used in the chemical ionization ion source.

(b) Unimolecular and CID Decomposition of Ion Clusters and Cluster Equilibria Measurements. It was mentioned in the Introduction that when ion clustering equilibria are measured using the neat clustering gas in the ion source, the desirable condition $f_{ex} << 1$ may not be present at the high-temperature end of the van't Hoff plots. In part II we described how $f_{ex}^{(n)}$ for $H_3O^+(H_2O)_n$ can be determined from eq 16. The high-temperature end for the present measurements was extended up to the point where the equilibrium constants had decreased to the value 0.1 $Torr^{-1}$, for $n = 3$, 4, and 5 (see Figure 2). The $f_{ex}^{(n)}(H_3O^+)$ at the corresponding temperatures are 0.015, 0.004, and 0.002, respectively. The earlier[15] evaluated $f_{ex}^{(n)}(K^+)$ for the same n and same condition ($K_{n-1,n} = 0.1$ $Torr^{-1}$) are 0.09, 0.3, and 0.6, respectively. Both sets of values must be considered only as approximate. Yet the differences between the two systems are sufficiently large to allow the conclusion that the conditions for the present measurements of $H_3O^+(H_2O)_n$ are safe, while this is not the case for the potassium system for $n > 4$.

In the earlier H_3O^+ work (Searles[10]) the measurements extended to $K_{n-1,n}$ as low as 0.01 $Torr^{-1}$. However, most of the experimental points were obtained for equilibrium constants higher than 0.1 $Torr^{-1}$ (see Figure 2). Therefore, the steeper slopes in the Searles' measurements also cannot be caused by too high values of f_{ex}.

The results in Figure 8 indicate that the $H_3O^+(H_2O)_5/H_3O^+(H_2O)_4$ ratio, if measured at ion-tube pressures in the $10^{-5} - 10^{-4}$ Torr range, will be strongly affected by CID. Not only will the detected ion intensity for $n = 5$ be significantly lowered by CID, but this lowering will increase with temperature. The net result will be an increase of the negative slope of the van't Hoff plot for the (4,5) equilibrium and $-\Delta H^0_{n-1,n}$ and $-\Delta S^0_{n-1,n}$ values which are too high. Of course, this instrumental artifact will also manifest itself in a lowering of the observed equilibrium constant $K_{n-1,n}$ with pressure (at constant temperature) in the vacuum system. Such an effect was observed in the present apparatus. Unfortunately, the mass analysis pressure in the Searles'[10] experiments was not recorded. We do not know whether in that vacuum system the residual pressure was high enough to cause significant CID error. The equilibrium constants in that work were found to be largely independent of ion source pressure. This would not have been the case had CID due to residual gas pressure been involved. Therefore we are not able to pinpoint the cause which affected the Searles'[10] measurements. Nevertheless, the present CID results in Figure 8 are of importance to ion-association equilibria measurements. They show that serious CID can occur if the vacuum system is above 10^{-5} Torr. Furthermore, because of the dependence of CID on the temperature of the ion source, the ion transmission does not only decrease with n but also with temperature.

Registry No. H_3O^+, 13968-08-6; $H_3O^+(H_2O)$, 22206-74-2; $H_3O^+(H_2O)_2$, 23108-28-3; $H_3O^+(H_2O)_3$, 12501-73-4; $H_3O^+(H_2O)_4$, 26719-17-5; $H_3O^+(H_2O)_5$, 40192-94-7; $H_3O^+(H_2O)_6$, 15690-19-4.

Energy Storage and Reaction Pathways in the First Step of the Vision Process

Arieh Warshel* and Natalia Barboy

Contribution from the Department of Chemistry, University of Southern California, University Park, Los Angeles, California 90007. *Received May 26, 1981*

Abstract: The energy storage, resonance Raman spectra, molecular structure, and pathways of formation of the first intermediate in the vision process (bathorhodopsin) are analyzed. The analysis involves a simulation of the protein constraint by an effective steric potential, assuming a limited relaxation of the protein cavity during the isomerization time. It is found that a reasonable estimate of the protein flexibility confines the isomerization pathway in a unique way and simulates the trapping of bathorhodopsin as a strained type intermediate. Adjusting the single parameter that represents the protein rigidity to simulate the energy storage and resonance Raman lines of bathorhodopsin leads to a quite unique prediction of its structure and explains the difference in quantum yield for the formation of bathorhodopsin from rhodopsin and isorhodopsin.

The first step of the vision process involves absorption of light by rhodopsin molecules and a very fast and efficient conversion to the intermediate bathorhodopsin (also known as prelumirhodopsin) (for a recent review, see ref 1). The chromophore of rhodopsin is a protonated Schiff base of retinal (PSBR) in the 11-cis conformation. The conformation of this chromophore in bathorhodopsin is not known, and its characterization is essential for detailed understanding of the primary event in the visual process. Fortunately, there are many experimental constraints that limit drastically the selection of models for this intermediate. These constraints include the following observations: (i) The formation of bathorhodpsin at 30 K takes less than 6 ps.[2] (ii) The quantum yield of this process is very high (0.7), even at 4 K.[3] (iii) The energy of bathorhodpsin is about 35 kcal/mol higher than that of rhodopsin (about 60% of the light energy is stored).[4] (iv) Special resonance Raman (RR) lines appear in the spectrum of bathorhodopsin.[5] (v) Isorhodopsin that includes 9-cis PSBR as a chromophore is converted by light to bathorhodopsin with low quantum yield.[3] (vi) The rate of formation of bathorhodopsin from deuterated rhodopsin is significantly slower than the corresponding rate when the protein is undeuterated.[2] Any detailed molecular model for bathorhodopsin should be capable of *simulating* these experimental facts. Thus, models of the first step

(1) Birge, R. R. *Annu. Rev. Biophys. Bioeng.* **1981**, *10*, 315.
(2) Peters, K.; Applebury, M. L.; Rentzepis, P. M. *Proc. Natl. Acad. Sci. U.S.A.* **1977**, *74*, 3119.
(3) Hurley, J. B.; Ebrey, T. G.; Honig, B.; Ottolenghi, M. *Nature (London)* **1977**, *270*, 540.
(4) Cooper, A. *Nature (London)* **1979**, *282*, 531.
(5) Oseroff, A. R.; Callender, R. H. *Biochemistry* **1974**, *13*, 4243.

0002-7863/82/1504-1469$01.25/0

of the vision process that involve cis–trans photoisomerization[6-11] should account for isomerization in a restricted active site of a protein at 4 K. On the other hand, models that do not involve cis–trans photoisomerization (model B of ref 11 and the models of ref 2 and 12) should explain how rhodopsin is eventually isomerized to the all-trans conformation if bathorhodopsin is still a cis-type molecule. The energy storage poses another major problem; storage of more than 15 kcal/mol was not simulated or explained in a consistent way by any of the previous works (see section II).

In this paper, we *assume* that the first step of the vision process involves cis–trans photoisomerization and try to examine the implications of such an assumption in terms of the above constraints.

Section I describes the introduction of the steric restriction of the protein as an effective potential and the use of this potential for evaluation of the amount of strain energy in bathorhodopsin. Section II considers the storage of electrostatic energy in bathorhodopsin and discusses some general aspects of energy storage by light-induced charge separation. Section III considers the effect of the protein cavity on the reaction pathways and quantum yield. It is shown that the steric constraint restricts severely the possible pathways and intermediates. Requiring our model to account for the observed energy storage and resonance Raman lines of bathorhodopsin, as well as for the formation of bathorhodopsin from both rhodopsin and isorhodopsin, leads to a prediction of the structure of bathorhodopsin.

I. Storage of Strain Energy in a Restrictive Active Site

Proteins are relatively compactly arranged molecules (having a specific volume of ~0.75 which is the same as the average specific volume of crystals of amino acids).[16] The size of the empty "cavities" in proteins is not likely to be larger than the size of a water molecule; larger cavities will be filled by water molecules. Thus, it is reasonable to assume that the chromophore in rhodopsin is surrounded by protein groups (or bound water molecules) and that these groups are likely to limit the possible isomerization pathways. This effect is particularly important during the formation of bathorhodopsin at low temperatures, where the time required for the protein groups to accommodate a new isomer is long compared to the time (<6 ps) required for photoisomerization. In order to examine the steric effect of the protein, we use an effective potential that simulates the constraint of the protein cavity. This potential is obtained by the following approach: The chromophore in its initial configuration (e.g., 11-cis for rhodopsin and 9-cis for isorhodopsin) is surrounded by a surface of close-packed spheres that interact with each other and with the chromophore by a 6–12 van der Waals potential with (ϵ^* = 1 kcal/mol and r^* = 3 Å). The surface spheres are allowed to reach the equilibrium configuration, $R^S{}_0$, which minimizes their interactions with the chromophore and each other. This generates a *relaxed* cavity around the chromophore, simulating the fact that protein cannot be significantly strained in the ground state of rhodopsin (otherwise the chromophore will not be bound to the protein). The constraint of the protein cavity on the deformations

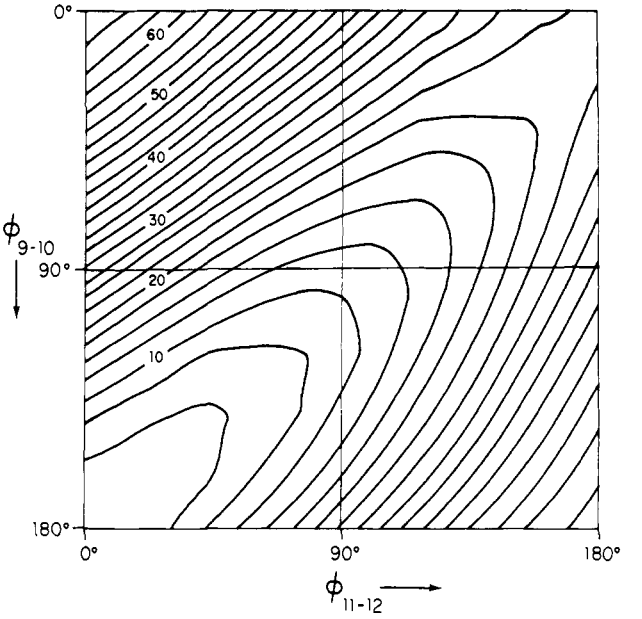

Figure 1. Constraint potential V_{cons} for protein cavity around the 11-cis-12-s-trans chromophore. The potential is calculated for K = 0.5 kcal mol^{-1} Å^{-2}. The indicated contour spacing is given in kcal/mol.

of the chromophore is represented now in terms of the equilibrium coordinates of the cavity, $R^S{}_0$, by the relation

$$V_{cons}(r,R^S) = V_{vdw}(R^S,r) + \tfrac{1}{2}\sum_i K(R^S{}_i - (R^S{}_0)_i)^2 \qquad (1)$$

where r and R^S are the coordinates of the chromophore and the cavity atoms, V_{vdw} is the van der Waals interaction between the chromophore and the cavity atoms, and K is the empirical force constant of the protein cavity. The last term in eq 1 introduces a restoring force that limits the shifts of the coordinates of the cavity atoms, R, from their original position, R_0. This term restricts indirectly the changes in the chromophore coordinates, r, since the cavity coordinates are coupled to the chromophore coordinates by the van der Waals term.

The upper limit for the value of the force constant K can be taken as 4 kcal mol^{-1} Å^{-2} which cooresponds to a storage of 2 kcal mol^{-1} Å^{-2} strain energy for a root mean square shift ($[\sum_i(\Delta r_i)^2]^{1/2}$) of 1 Å in the coordinates of the chromophore. This value of K is based on an estimate of the upper limit of storage of strain energy, obtained from calculations of the relaxations of lysozyme[18] and hemoglobin[19] as a result of root mean square shifts of less than 1 Å in their prosthetic groups. However, the effective value of K in rhodopsin is expected to be smaller since it corresponds to a much largely geometry change. That is, the large shifts of the chromophore atoms are expected to exert strong forces on the protein cavity and the resulting protein relaxation will be larger than that predicted by calibrating the harmonic approximation of eq 1 on cases of small shifts. Thus we take here the cavity force constant K as a variable parameter, examine the upper and lower limits for its effect, and use the observed energy storage for determination of the proper K for studying the reaction pathways.

The overall potential of the protein–chromophore system is given by

$$V^M = V_{intra}{}^M + V_{cons} + V_{elect} \qquad (2)$$

where $V_{intra}{}^M$ is the intramolecular potential of the isolated chromophore in the Mth electronic state, V_{cons} is the potential of the steric constraint (eq 1), and V_{elect} is the electrostatic interaction between the chromophore and the protein (see section II). Since the forces due to $V_{intra} + V_{cons}$ (which are referred to here as "steric forces") are stronger than those due to the electrostatic potential,

(6) Warshel, A. *Nature (London)* **1976**, *260*, 679.
(7) Rosenfeld, T.; Honig, B.; Ottolenghi, M.; Hurley, J.; Ebrey, T. G. *Pure Appl. Chem.* **1977**, *49*, 341.
(8) Weiss, R. M.; Warshel, A. *J. Am. Chem. Soc.* **1979**, *101*, 6131.
(9) Birge, R. R.; Hubbard, L. M. *J. Am. Chem. Soc.* **1980**, *102*, 2195.
(10) Honig, B.; Ebrey, T.; Callender, R. H.; Dinur, U.; Ottelenghi, M. *Proc. Natl. Acad. Sci. U.S.A.* **1979**, *76*, 2503.
(11) Warshel, A. *Proc. Natl. Acad. Sci. U.S.A.* **1978**, *75*, 2558.
(12) Lewis, A. *Proc. Natl. Acad. Sci. U.S.A.* **1978**, *75*, 549.
(13) Warshel, A. "Modern Theoretical Chemistry"; Segal, G., Ed.; Plenum: New York, 1977; Vol. 7.
(14) Warshel, A.; Levitt, M. *QCPE* **1974**, *274*.
(15) Warshel, A.; Lappicierella, A. *J. Am. Chem. Soc.* **1981**, *103*, 4664.
(16) Richards, F. M. *Annu. Rev. Biophys. Bioeng.* **1977**, *6*, 151.
(17) The calculations presented in Table I kept the distance between the counterion and the chromophore constant in order to separate the electrostatic and steric contributions. More defined calculations that allow the distance to increase during the isomerization process gave large contribution of the resonance form II and a shallow V_{intra}. This result is obtained even without placing a negative charge near the β-ionone ring.[11]

(18) Warshel, A.; Levitt, M. *J. Mol. Biol.* **1976**, *103*, 227.
(19) Warshel, A.; Weiss, R. M. *J. Am. Chem. Soc.* **1981**, *103*, 6131.

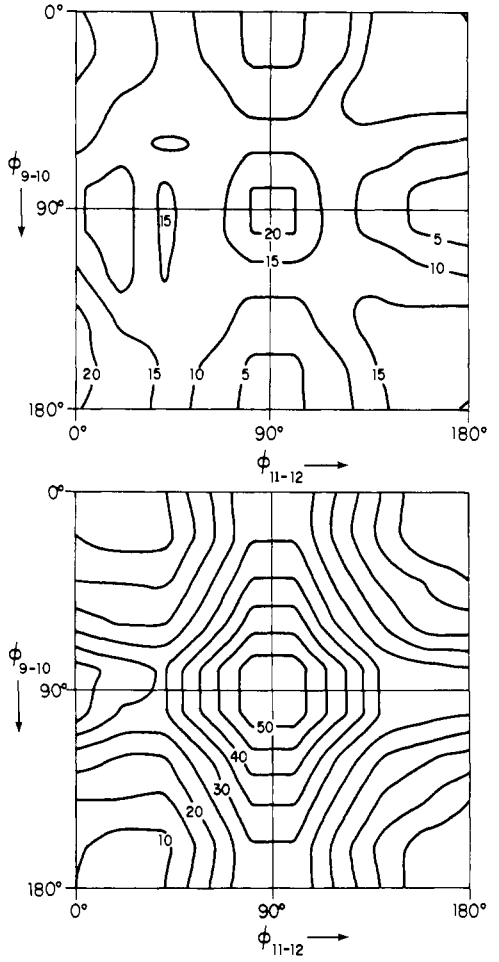

Figure 2. Intramolecular potential, V_{intra}, for the excited (up) and ground (down) PSBR. The indicated contour spacing is given kcal/mol.

we consider first the effects of the steric forces.

The behavior of V_{intra} and V_{cons} in the multidimensional space of the system was examined by using the adiabatic mapping method,[13] where the potential $V_{intra} + V_{cons}$ was minimized with respect to all Cartesian coordinates of the system for fixed values of ϕ_{9-10} and ϕ_{11-12}. The resulting contribution of V_{cons} is presented in Figure 1. This contribution was obtained by using $K = 0.5$ kcal mol^{-1} Å^{-2} and the V_{intra} of the excited electronic state. Using V_{intra} of the ground state gives a somewhat different V_{cons} since the least energy values of the various torsional angles (e.g., ϕ_{10-11}) are different. However, the main features are the same; the constraint potential favors motions along the diagonal of the ϕ_{9-10}, ϕ_{11-12} potential surface ($\phi_{9-10} + \phi_{11-12} \simeq 180°$).

The calculated V_{intra} for the ground (G) and the lowest excited state (E) of the PSBR are presented in Figure 2. These potentials were obtained by the QCFF/PI method[13-15] using single and double configuration interactions.[25] The results of the adiabatic mapping for the ground- and excited-state surfaces of $V_{intra}^{M} + V_{cons}$ are presented in Figures 3 and 4. As seen from these figures the combination of the constraint potential (which favors concerted motion of two angles) and the intramolecular potentials (that favors torsion of only one angle) leads to a compromise, where the least energy motion involves rotation of ϕ_{11-12} up to 90° accompanied by a rotation of ϕ_{9-10} to about 150°. This partially concerted motion minimizes the chromophore–protein steric interaction while avoiding the intramolecular barrier at $\phi_{9-10} = 90°$, $\phi_{11-12} = 90°$. When ϕ_{11-12} reaches 90° the excited chromophore crosses to the ground state with high probability retaining its direction toward the trans configuration of the 11–12 bond.[8] The least energy pathway for the ground-state relaxation of the chromophore involves a large shift of the C_{13} methyl group, which is being hindered by the steric resistance of the protein (see molecular drawing in Figure 3). The interplay between the tendency of the chromophore to reach a planar trans configuration and the steric resistance of the protein determines the conformation of the bathorhodopsin intermediate. This point is demonstrated in Table I, which gives $V_{intra}^{G} + V_{cons}$ for various possible values of K. As seen from Table I and Figures 3 and 4, a very conservative estimate of $K = 0.25$ kcal mol^{-1} Å^{-2} leads to the trapping of a twisted intermediate ($\phi_{11-12} = 140°$, $\phi_{9-10} = 150°$) with ~25-kcal/mol strain energy. The possibility that bathorhodopsin is a twisted trans-type intermediate becomes even more appealing when one considers the increase in the relative stabilization of the resonance form II as a result of cis–trans isomerization that takes

Table I. Storage of Strain Energy[a]

ϕ_{11-12}	ϕ_{9-10}	V_{intra}^{G}	$[\sum_i \Delta r_i^2]^{1/2}$	$V_{intra}^{G} + V_{cons}$		
				$K = 1$	$K = 0.5$	$K = 0.25$
90	140	35.3	6.3	[55.5]	45.5	40.3
100	140	30.1	7.7	60.1	54.1	37.5
110	150	25.4	8.3	60.4	42.9	34.1
120	150	20.2	9.0	60.5	40.4	30.2
130	150	15.3	10.0	65.5	[40.3]	27.8
140	150	10.5	10.9	70.5	40.5	[25.5]
150	160	10.6	11.8	80.6	45.6	28.1
160	160	5.5	12.2	80.5	43.0	24.2
180	180	0.0	13.0	85.0	42.5	21.2

[a] Energies in kilocalories/mole and angles in degrees. The constraint force constant, K, is given in kcal mol^{-1} Å^{-2}. The table gives the sum of the ground-state intramolecular potential and the constraint potential ($V_{intra}^{G} - V_{cons}$) for the indicated value of ϕ_{11-12} and ϕ_{9-12} (where the energy is minimized with respect to all other degrees of freedom). For each K we indicate in bracket the energy stored in the corresponding equilibrium geometry. The root mean square shifts $[\sum_i \Delta r_i^2]^{1/2}$ are also given (in Å) for each of the indicated configuration.

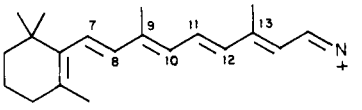

I

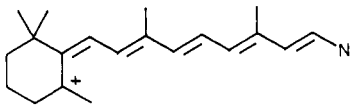

II

the protonated Schiff base away from its negative counterion.[17] This case involves a significant bond alternation that leads to a "flattening" of V_{intra}^{G} and allows for trapping of a twisted trans-type intermediate by weak steric forces of the protein.

Storage of a significant amount of strain energy seems to be in a clear contradiction to the results of previous studies of the energetics of lysozyme[18] and hemoglobin.[19] These studies have placed a limit of less than 2 kcal/mol on the storage of strain energy. However, in hemolglobin and lysozyme the geometries of the prosthetic groups change by less than 1 Å during the reaction. Here, on the other hand, the "least displacement" pathway of the chromophore involves a root mean square displacement (Table I) of $\{\sum_i (\Delta r_i^2)\}^{1/2} > 10$ Å for $\phi_{11-12} = 10° \rightarrow \phi_{11-12} = 150°$. Note that the strain energy is stored only at low temperature (<133 K) where the protein conformational relaxation (bathorhodopsin → lumirhodopsin), which can release the strain, is frozen. In fact, since the energy of protein unfolding is less than 15 kcal/mol in most proteins, strain energy cannot be stored for a long period of time at room temperature.

II. Storage of Light Energy as Electrostatic Energy

Storage of light energy by light-induced isomerization that separates the positively charged end of the PSBR from a negatively charged carboxylic acid of the protein was proposed before.[6,8,10,20]

(20) Warshel, A. *Photochem. Photobiol.* **1979**, *30*, 285.

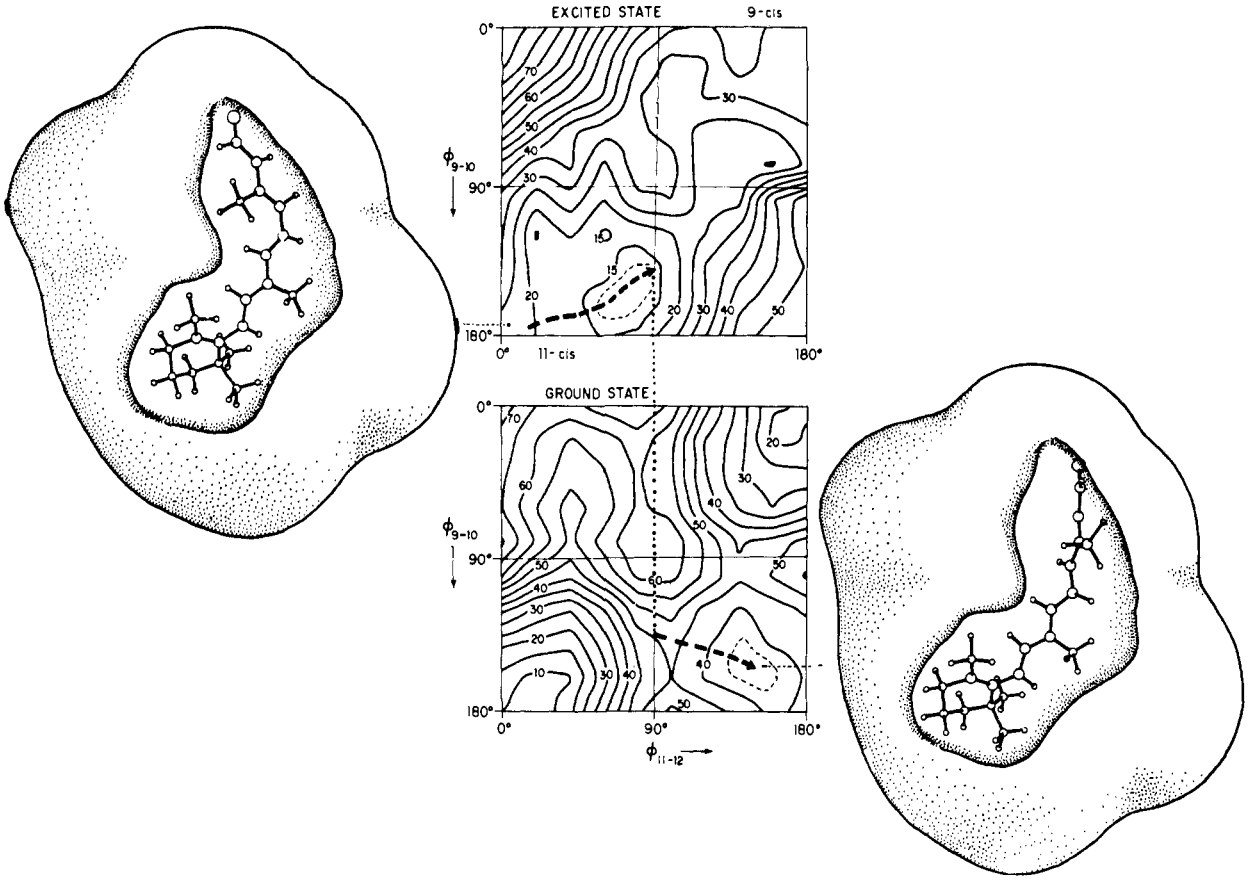

Figure 3. Superposition of V_{intra} and V_{cons} for the excited (up) and ground (down) potential surfaces. The indicated contour spacing is given in kcal/mol. The figures shows the pathway for formation of bathorhodopsin from rhodopsin.

In order to consider the validity of such proposals, we have to clarify several conceptual problems. The most serious problem arises from the suggestion of ref 10 that in rhodopsin the $NH^+\cdots COO^-$ ion pair is situated in an hydrophobic (low dielectric) environment where a change in the distance between the charges (e.g., from 3 to 5 Å) can store ~40 kcal/mol. Unfortunately, the proposal of an hydrophobic site for the ion pair is inconsistent with one major fact: ion pairs are *not* stable in low dielectric environments (see ref 22 for discussion), and the $=NH^+\cdots COO^-$ pair will be converted to $=N\cdots COOH$ (the reader can best realize this point by considering the related fact that amino acids cannot exist in their zwitterionic forms in nonpolar solvents). Thus the $NH^+\cdots COO^-$ ion pair in rhodopsin can exist only in a polar environment being "solvated" by the permanent dipoles of the protein.[21] This, however, presents another basic problem; it is very difficult to store significant energy by charge separation in a polar environment.[21,22] This dilemma can be resolved if the isomerization takes the protonated Schiff base from a polar environment to a nonpolar environment (Figure 5) (also see ref 20). This novel mechanism is quite different from common mechanisms in physical organic chemistry which involve processes in either polar or nonpolar environments.

The amount of electrostatic energy stored by the mechanism of Figure 5 can be calculated for assumed models by microscopic dielectric approaches.[18,22,24] However, since the structure of the protein is not known, we estimate this energy using the following considerations: The solvation energy of a charged group in a polar solvent should be similar (within 5 kcal/mol) to the solvation energy of the same group by protein dipoles and/or charges at equilibrium conditions[20,22] (this is evident by the fact that the pK_a's of ionizable groups in proteins, at equilibrium conditions, are similar within a few units to the corresponding pK_a's in solutions). Thus, the solvation energy of the Schiff base edge in rhodopsin should be similar to its solvation in water. Therefore, the energy stored by the charge separation mechanism of Figure 5 can be approximated by the energy change upon moving the protonated Schiff base from a polar to a nonpolar environment (Figure 6). The corresponding energy difference can be estimated by using the Born formula[23] which gives the solvation free energy of a charge Q in a solvent cavity of effective radius $\bar{a}$ as

$$G_{sol} = -166(Q^2/a)[1 - (1/\epsilon)] \quad (3)$$

where the solvation free energy, G_{sol}, is given in kcal/mol, and

(21) Warshel, A. *Proc. Natl. Acad. Sci. U.S.A.* **1978**, *75*, 5250.
(22) Warshel, A., *Biochemistry* **1981**, *20*, 3167.
(23) Born, M. *Z. Phys.* **1920**, *1*, 45.
(24) Warshel, A. *J. Phys. Chem.* **1979**, *83*, 1640.
(25) The present calculation gave a barrierless excited state. Different parameters can give up to a 5 kcal/mol barrier. Thus it is not clear if the excited-state barrier for isomerization in solution[8] is due to the solvent or the chromophore. The effect of the solvent and the protein on the barrier requires further study. However, if the primary event is cis–trans isomerization, then it is clear that no excited-state barrier exists in the protein.

(26) The formalism of ref **9** may lead to suggestion that the quantum yield for a barrierless photoisomerization can be smaller than 0.5 if the first trajectory that crosses the **90°** region has a large amount of excess vibrational energy (e.g., energy in stretching modes). This is inconsistent with the more complete model of ref 6 which included all molecular vibrations in its trajectory calculations. This inconsistency might be due to the semiclassical expression of ref 9 which includes in its energy gap, ΔW, a fraction of the excess vibrational energy. A more correct expression should scale the transition probabilities of channels which involve changes in vibrational quantum numbers by the corresponding Franck–Condon factors.[34] Such a treatment will reduce drastically the probability of transitions from excited vibrations of excited electronic states to ground-state vibrations of ground electronic states. Thus, the main channels for transitions from excited vibrations of the excited electronic state will be to excited vibrations (with similar vibrational quantum numbers) of the ground electronic state. The effective energy gap for these transitions *should not* include the vibrational excess energy. For example, if a molecule with $n = 2$ for a C–H stretch will cross along the torsional coordinate to the ground electronic state its C–H stretch will stay at $n = 2$.

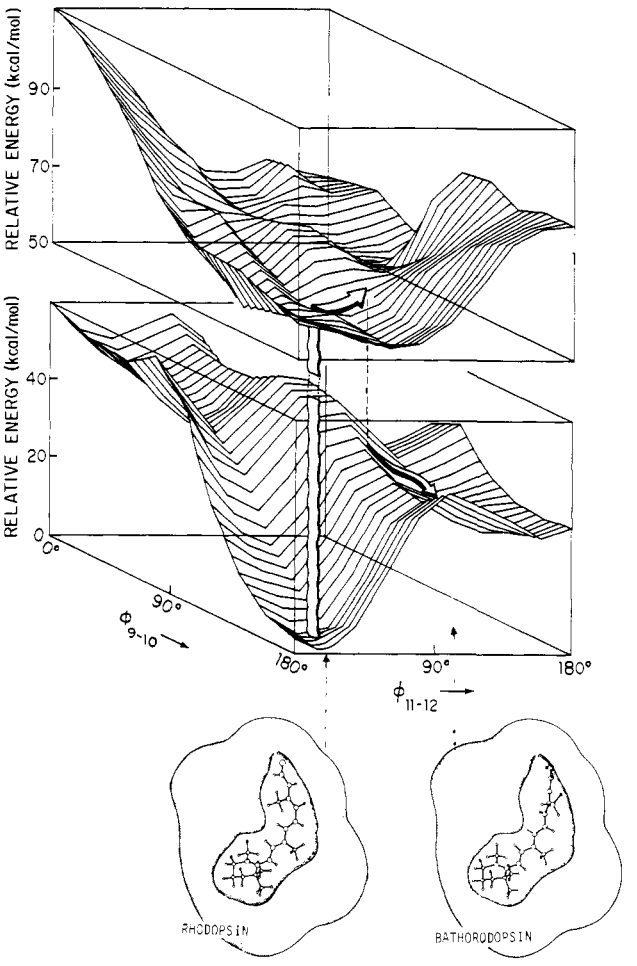

Figure 4. Three-dimensional representation of $V_{intra} + V_{cons}$ for the ground and excited state. The figure shows the pathway for formation of bathorhodopsin and its trapping as a twisted intermediate.

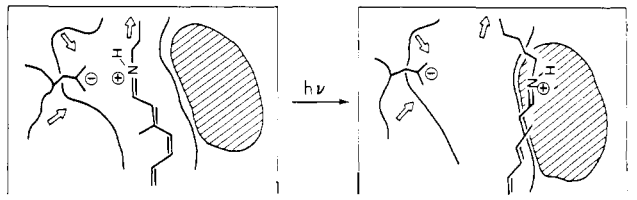

Figure 5. Light-induced charge separation as a result of cis–trans photoisomerization. The positively charged nitrogen edge of the molecule is moved from the polar environment, of the negatively charged ionized acid and the stabilizing protein dipoles, to a nonpolar environment (cross hatched region). This process can store a significant amount of energy.

ϵ is the bulk dielectric constant. According to eq 3 the solvation free energy of charges in nonpolar environment ($\epsilon \sim 2$) is only about half of the corresponding solvation in a polar environment ($\epsilon > 10$). Since the solvation energy of a protonated Schiff base in polar solvents is calculated by the SCSSD model[24] to be $\sim$−60 kcal/mol, the solvation free energy in a nonpolar environment should be about −60/2 = −30 kcal/mol. Thus, we conclude that the electrostatic energy stored by moving the positively charged end of the PSBR from a polar to a nonpolar environment can be about 30 kcal/mol. This storage of electrostatic energy can be viewed as a change of $\sim$22 units in the local pK_a's of the Schiff base and the ionized acid (eq 5 of ref 20).

The above considerations bring us to an interesting problem. Usually proteins do not store significant energy by changes in pK_a's at equilibrium conditions, since they tend to unfold rather than to bury charges in a nonpolar environment.[22] However, as was argued in ref 20, the complete relaxation of the protein dipoles can be sufficiently slow to allow for large changes in local pK_a's and a significant energy storage during times of the order of

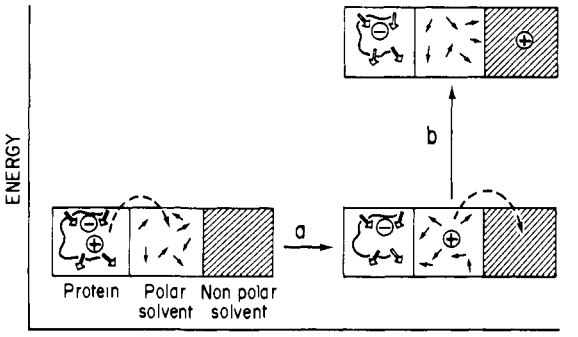

Figure 6. Estimating the amount of electrostatic energy stored by the charge separation mechanism of Figure 5. As argued in the text the change in solvation energy upon moving the protonated Schiff base from the protein to a polar solvent (step a) is small. Thus the overall energy stored in the process described in Figure 5 can be estimated by evaluating the energy of transferring the protonated Schiff base from a polar to a nonpolar solvent (step b).

microseconds at room temperature. At low temperature, the protein relaxation can be frozen for a much longer period of time.

The possibility of storage of a large amount of electrostatic energy does not exclude the possibility of storage of a large amount of strain energy. That is, the least energy pathway of Figure 3 and Table I involves only about 1-Å shift of the Schiff base nitrogen from its initial position. This motion (that stores about 40-kcal/mol strain energy for $K = 0.5$, and 25 kcal/mol for $K = 0.25$) is not expected to store a large amount of electrostatic energy. However, if the protein relaxation is larger than that estimated in our calculations (e.g., the effective K approaches 0.1 kcal mol^{-1} Å^{-2}), then the change in the distance between the charges is expected to be larger, storing a large amount of electrostatic energy and only a small amount of strain energy. It is quite possible that bathorhodopsin stores a large part of its excess energy as strain energy and that this energy is converted to electrostatic energy upon formation of the next intermediate, lumirhodopsin. It is also possible that the formation of bathrhodopsin involves two successive steps: a very fast one (10^{-12} s) where a significant part of the light energy is stored as strain energy and a somewhat slower relaxation step ($\sim 5 \times 10^{-12}$ s) that converts the strain energy into electrostatic energy.

An interesting experimental information about the relaxation of the ground-state energy is given by the isotope effect on the rate of formation of bathorhodopsin.[2] This isotope effect is most probably due to a ground state proton transfer between two groups of the protein[11] following pK_a changes as a result of the light-induced charge separation (a discussion of a related case in the first step of the action of bacteriorhodopsin is given in ref 20). The proton-transfer process may provide a simple channel for electrostatic energy relaxation.

III. Reaction Pathways and Quantum Yields

The discussion in the previous section demonstrates how the energy of bathorhodopsin may be stored. Another crucial unresolved problem is the difference between the quantum yields of the rhodopsin → bathorhodopsin and the isorhodopsin → bathorhodopsin reactions, which are $\sim$0.7 and <0.3, respectively.[3] An interesting clue to this problem emerges from the calculations of the constraint for isomerization in the cavity defined by the 9-cis chromophore (R^S_0 is evaluated by building a cavity around the 9-cis isomer). This constraint (Figure 7) was obtained by adiabatic mapping of $V_{cons} + V_{intra}{}^E$. A somewhat different potential is obtained for adiabatic mapping of $V_{cons} + V_{intra}{}^G$, but in both cases the constraint increases much faster with torsional motion than the constraint for torsional motion in the cavity defined by the 11-cis chromophore. This is due to the fact that a torsion around the 9–10 bond involves a larger geometry change (and larger steric resistance by the protein) than a torsion around the 11–12 bond. At a first glance this difference in steric constraint does not seem to account for the difference in quantum yields. That is, as argued in ref 27, excited-state torsion to $\phi_{9-10} = 90°$

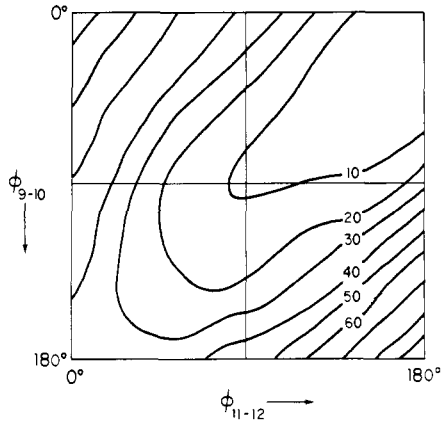

Figure 7. Calculated constraint potential, V_{cons}, for the protein cavity around the 9-cis chromophore. The potential is calculated for $K = 0.5$ kcal mol^{-1} Å^{-2}. The indicated contour spacing is in kcal/mol.

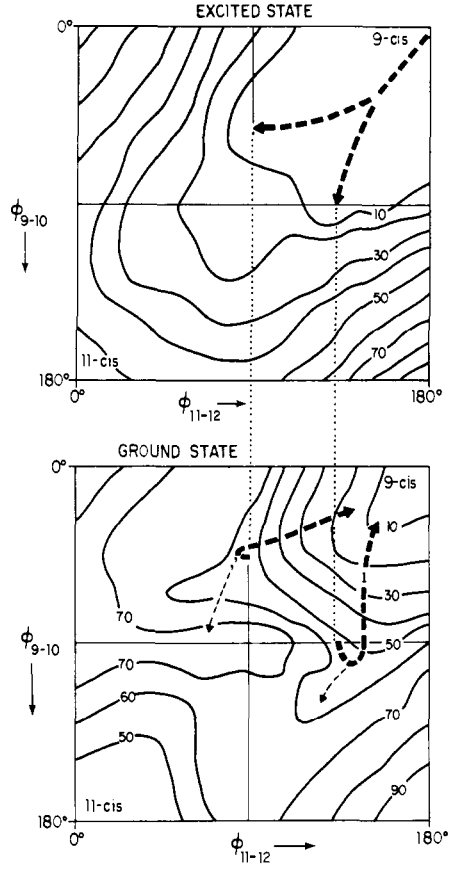

Figure 8. Superposition of the constraint potential, V_{cons}, for the cavity around the 9-cis chromophore and the intramolecular potential, V_{intra}, for the excited (up) and ground (down) states. The indicated contour spacing is in kcal/mol. The figure shows the pathways for the photoisomerization of isorhodopsin (see text for discussion).

is not prevented by the steric potential of the protein, and according to the concepts of ref 8 the quantum yield for photoisomerization on a barrierless excited state should be about 0.7 and not the observed value of <0.3.[26] However, as shown schematically in Figure 8, an isomerization trajectory that retains its direction during the surface-crossing process can reverse its direction on

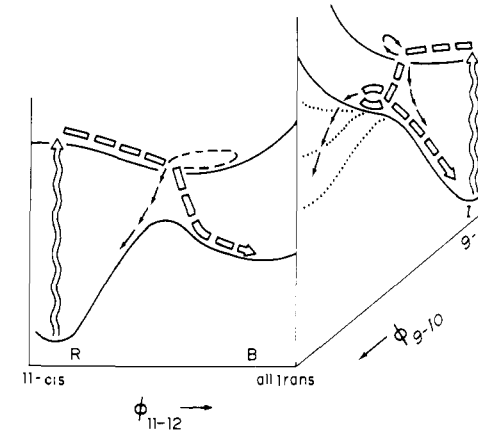

Figure 9. Schematic depiction of the relation between the protein constraint and the quantum yields for the rhodopsin → bathorhodopsin (R → B) reaction and the isorhodopsin → bathorhodopsin (I → B) reactions. In the R → B reaction 50% of the molecules cross to the ground state in the first pass at the 90° region and continue toward the trans region (see ref 8 for details). In the I → B reaction most of the trajectories that cross to the ground state are deflected back to the 9-cis region by collision with the protein cavity. Some of the trajectories that pass the 90% region "push" the protein, force its cavity to relax, and eventually reach the B region. The time-dependent relaxation of the protein potential as a response to the strong steric forces of the chromophore is indicated by the family of dotted potentials. This shows how the motion of the chromophore toward the B region changes the protein potential that was obtained with $K = 0.5$ kcal mol^{-1} Å^{-2} to potentials that correspond to small K's and a more significant protein relaxation.

the ground state as a result of collision with the protein cavity. The probability of deflection of the trajectories on the ground state is much larger for isomerization of isorhodopsin than for rhodopsin (compare Figure 3 to Figure 8).

The relation between the photoisomerization pathways of rhodopsin and isorhodopsin are summarized in Figure 9. In the rhodopsin → bathorhodopsin photoisomerization, all the excited-state trajectories reach the surface-crossing region at $\phi_{11-12} = 90°$, $\phi_{9-10} = 140 \pm 20°$. This pathway is unique since the ground-state chromophore in rhodopsin is already twisted around the 11–12 bond by 10° or more (due to the steric repulsion between the C_{13} methyl and the H_{10} proton). On the other hand, the chromophore in isorhodopsin can move toward the all-trans (bathorhodopsin), the 9-cis-11-cis, and the 11-cis (rhodopsin) configurations. Apparently the protein steric strain deflects back most of these trajectories when they cross to the ground state and probably restricts the number of excited-state trajectories that reach the 90° region. The experimentally observed quantum yield indicates that less than 30% of the trajectories lead to formation of bathorhodopsin (a very small percent might reach the rhodopsin region[32]). The least energy pathway from isorhodopsin to bathorhodopsin is not entirely apparent from Figure 8. That is, the twist of ϕ_{9-10} to 90° requires (in addition to the twist of ϕ_{11-12})

(27) The small temperature dependence for the isorhodopsin → bathorhodopsin transition indicates that the corresponding excited-state barrier is very small (less than 0.2 kcal/mol). Furthermore, the observation of a very short (picoseconds) time for return to the ground state of isorhodopsin upon excitation of isorhodopsin[28] indicates that the chromophore reached the region of $\phi_{9-10} = 90°$ (which is the only region where the surface crossing is efficient enough to give a lifetime of 10^{-12} s[8]).

(28) Applebury, M. L. *Photochem. Photobiol.* **1980**, *32*, 425.
(29) Warshel, A., *Ann. Rev. Biophys. Bioeng.*, *6*, 273 (1977).
(30) Eyring, G.; Curry, B.; Mathies, R.; Fransen, R.; Palings, I.; Lugtenburg, J. *Biochemistry* **1980**, *18*, 2410.
(31) Eyring, G.; Curry, B.; Mathies, R.; Broek, A.; Lugtenburg, J. *J. Am. Chem. Soc.* **1980**, *102*, 5390.
(32) A concerted rotation around the 9–10 and 11–12 bonds have been suggested[6] as one of the *two* pathways between isorhodopsin and bathorhodopsin (the second was a concerted rotation about the 9–10 and 15–16 bonds). Photostationary absorption measurements of the two almost overlapping peaks of isorhodopsin and rhodopsin were used to exclude the concerted 9–10, 11–12 isomerization[7] of isorhodopsin. It seems now from time-resolved resonance Raman studies[33] that this channel is open. It should be noted, however, that the isomerization around the 9-cis bond is anyhow of secondary importance since it is largely blocked by the protein steric effect and in some pigments the quantum yield for the isorhodopsin → rhodopsin reaction is less than 0.1.
(33) Hayward, G.; Carlsen, W.; Siegman, A.; Strayer, L. *Science (Washington, D.C.)* **1981**, *211*, 942.
(34) Warshel, A. *J. Phys. Chem.*, in press.

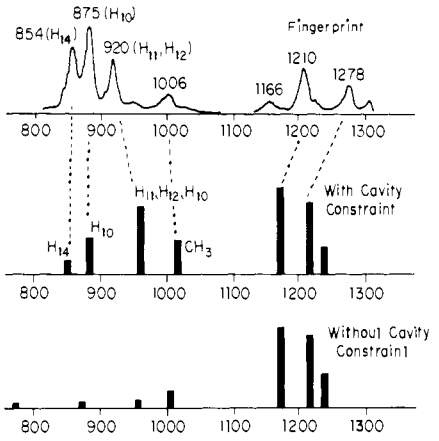

Figure 10. Observed RR spectrum of bathorhodopsin[30] (upper figure) and the calculated RR lines of the bathorhodopsin model with and without the cavity constraint (middle and lower figures).

a twist of ϕ_{7-8} to less than 150° to minimize collisions with the protein cavity. At the ground state, when the value of ϕ_{9-10} increases to ~140°, the value of ϕ_{10-11} starts to decrease and reaches ~160° as the chromophore approaches the bathorhodopsin conformation. It will be of great interest to examine whether or not molecular dynamics calculations that involve the chromophore in a protein cavity can reproduce the complicated motion of the isorhodopsin → bathorhodopsin photoisomerization. It seems extremely unlikely that a simple rigid isomerization around the 9–10 bond, such as the one suggested in ref 7 and 9 (which would lead to root mean square geometry change of more than 20 Å), can account for the formation of bathorhodopsin from rhodopsin at low temperature.

Note that the potential presented in Figures 8 and 9 should be viewed as a time-dependent potential, where those trajectories that proceed from the isorhodopsin region to the bathorhodopsin region involve protein relaxation that eventually leads to the same (or similar) protein configuration obtained upon the rhodopsin → bathorhodopsin isomerization. This implies that after sufficient relaxation time the potential in the $\phi_{11-12} = 150 \pm 30°$, $\phi_{9-10} = 150 \pm 30°$ region in Figure 8 will approach the corresponding potential in Figure 3.

IV. Resonance Raman and Structural Constraints

The RR spectrum of bathorhodopsin contains special intense lines in the 800–1000-cm^{-1} region.[5,29,30] It has been proposed in ref 29 that these lines are due to a strained trans-type chromophore. This proposal was based on our calculations of the RR spectrum of trans-type PSBR, contraining the N···C_5 distance to stay close to its value in 11-cis, 12-s-trans PSBR (this simulates in a very rough way the protein constraint). Our past calculations could not, however, *reproduce* the lines in the 800–1000-cm^{-1} region with more than 10% of their observed relative intensity. Calculations that assume *artificial* geometry changes upon excitation[29,30] were more successful, but all attempts to *reproduce* such geometry changes by minimizing the ground and excited states of a given model of the chromophore have failed. Thus, it had seemed unlikely that the RR spectrum, which reflects geometry changes upon excitation,[29] could be used for determining the ground-state geometry of bathorhodopsin. This seems particularly disappointing in view of the successes of careful experimental studies[31] (which involve deuterium substitution of the different hydrogens of the chromophore) to assign the special lines as out-of-plane motions of the H_{10}, H_{11}, H_{12}, and H_{14} hydrogens. Realizing, however, that the present work restricts, dractically, the ground-state conformations of bathorhodopsin, we tried once more to calculate the RR spectrum, but this time in the presence of the protein constraints. The calculations which are summarized in Figure 10 reproduced, for the first time, the relative total intensity of the special lines without *assuming* the geometry change upon excitation. The relative intensity of H_{10}, H_{11}, and H_{12} lines is strongly dependent on the equilibrium geometry of the chromophore which depends on the constraint parameter K. The conformation that gave the best intensity pattern is presented in Figure 11 and Table II. Table II also presents the calculated geometry change upon excitation. Although trial and error model calculations of the type used here cannot be used to establish a unique prediction of the ground-state geometry, it is important to note that none of our previous model calculations could reproduce this geometry change until the introduction of the protein constraint. We realize that much more work should be done in refining the calculated RR spectrum of the individual lines, but we feel that the introduction of the protein constraint is a key step in this direction.

Table II. Ground and Excited State Conformation of the Bathorhodospin Model[a]

torsional angle	value in ground state	value in excited state
5–6	172	171
5–7	325	329
7–8	184	184
8–9	173	171
9–10	150	141
10–11	162	170
11–12	145	138
12–13	163	166
13–14	164	160
14–15	181	178
15–16	144	141

[a] Torsional angles in degrees. The calculations were done for cavity constraint of 0.25 kcal mol^{-1} Å^{-2} that stores 25-kcal/mol strain energy.

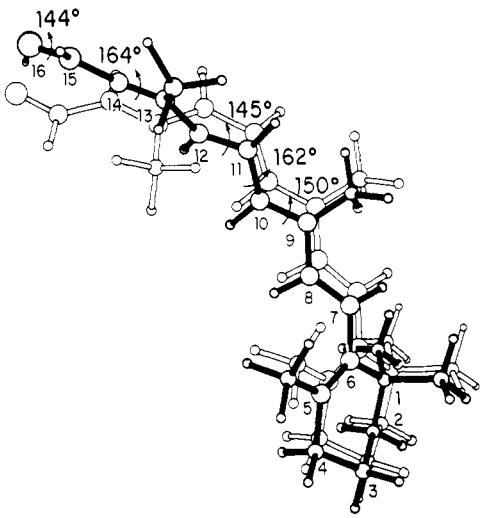

Figure 11. Calculated equilibrium geometries of the ground (solid) and excited states of the present model of bathorhodopsin. The calculated values of the torsional angles of the ground state are also indicated in the figure.

V. Concluding Remarks

The present work considers the effect of the steric constraints of the protein active site on the reaction pathways and energy storage during the first step of the vision process. Assuming a limited relaxation of the protein cavity during the isomerization time, we find that the protein confines the possible isomerization pathways in a unique way, where rotation around the 11–12 bond is concerted, with partial twisting of the 9–10 and other bonds. A simple isomerization around only one bond[7,9] will lead to collisions of the chromophore with the protein cavity which would prevent isomerization at low temperature.

Although there is no direct structural information about bathorhodopsin, it appears that the cross-information from several independent experiments provides a very narrow class of possible structures: The introduction of the protein steric constraint and the requirement that any valid model would simulate the energy

storage and the isomerization quantum yields seems to leave the model presented in Table II and Figure 11 as the most reasonable model. Of course, this model does not apply to the unlikely possibility that the first step of the vision process does not involve isomerization.

The present analysis of the energy storage in bathorhodopsin provides, for the first time, a *consistent* simulation of storage of a large amount of excess energy. It is shown that a very conservative estimate of the rigidity of the protein simulates trapping the chromophore in a strained conformation that stores a significant amount of energy. It is also shown how a light-induced charge separation can store about 30 kcal/mol if the protonated nitrogen is moved to a nonpolar region of the protein. It is suggested that a large amount of steric energy is likely to be converted into electrostatic energy during the ground-state relaxation of the protein.

The static constraint potential used in this work is only a rough approximation for the ad hoc assumption that the isomerization time is faster than the protein relaxation time. It is clear that a more complete study must involve molecular dynamics simulations of a chromophore in a protein cavity. However, preliminary molecular dynamics studies of the photoisomerization of the chromophore in a cavity of van der Waals molecules have indicated that the protein cavity does restrict the possible isomerization pathways. This point is strongly supported by the fact that the present work could provide a consistent analysis of the relation between the steric constraint of the protein and the quantum yields of formation of bathorhodopsin from rhodopsin and isorhodopsin.

The present model can be considered as a refinement of the previously proposed "bicycle-pedal" model.[6] The bicycle-pedal model simulated the primary event as a cis-trans isomerization around the 11-12 bond accompanied by a rotation around the 15-16 bond (see caption of Figure 2 in ref 6 and Figure 4 of ref 6). Introduction of the protein constraint suggests that the protein cavity prevents a complete rotation around the 15-16 bond due to its resistance to the displacement of the C_{13} methyl. Therefore, the isomerization around the 11-12 bond is accompanied by about 40° twist around both the 9-10 and 15-16 bonds, but the overall pathway is not drastically different from the bicycle-pedal pathway.[32] The key element in both models is that only a concerted twist of two or more bonds can lead to isomerization which will not be blocked by the "viscosity" of the protein cavity at low temperature. The presence of the protein constraints tends to confine the chromophore to concerted twists (along the diagonal of diagrams such as Figure 1) of two angles or more. On the other hand, the intramolecular excited-state potentials (Figure 2) imposes a small barrier for an entirely concerted motion when two angles reach the 90° range at the same time. Thus the isomerization motions should reflect a compromise between the inter- and intramolecular potentials where one angle, e.g., ϕ_{11-12} moves to 90° and another angle, or angles, are twisted by no more than 60°.

Acknowledgment. This work was supported by Grant EYO 1760 from the National Eye Institute. A. Warshel is an Alfred P. Sloan Fellow.

Molecular Orbital Constrained Electron Diffraction Studies. 4. Conformational Analysis of the Methyl Ester of Glycine

V. J. Klimkowski, J. D. Ewbank, C. Van Alsenoy,† J. N. Scarsdale, and Lothar Schäfer*

Contribution from the Department of Chemistry, University of Arkansas, Fayetteville, Arkansas 72701. *Received October 15, 1981*

Abstract: The electron diffraction data of the methyl ester of glycine were recorded at 75 °C in order to determine the conformational ground state of the system. The data were analyzed by using geometrical constraints (differences between closely spaced bond distances and bond angles) taken from a previous ab initio MO (4-21G) geometry optimization. On the basis of this analysis it must be concluded that the extended form of the system (I) is the most stable one. The presence of a small concentration (of a few percent) of a second conformer, the semiextended form (II), in the vapors of the compound at 75 °C, can also be inferred from the data. However, because of its dependence on the values of unknown amplitudes of vibration, the existence of measurable amounts of II at 75 °C cannot be established with certainty.

Introduction

The rationale for studies of this kind is based on the contention that, in conformational analyses, it should be advantageous to combine the results of quantum mechanical geometry optimizations with gas electron diffraction data. This is so because the relationship between ab initio calculations and gas electron diffraction is now to some extent complementary. Ab initio calculations can predict rather accurately the primary geometries (bond distances and angles) of simple organic molecules, but they are unreliable in determining small conformational energy differences because of basis set effects, electron correlation, and vibrational effects. Gas electron diffraction (GED), on the other hand, can provide a great deal of conformational information for unperturbed molecules, but this information is often difficult to decipher, because it may be correlated to small differences in primary structural parameters which are not resolved in the data. Assumptions concerning such differences therefore often have to be introduced into GED investigations and can make the results obtained in this way somewhat unreliable.

In molecular orbital constrained electron diffraction (MOCED) studies, those results from quantum mechanical geometry optimization which can be trusted, namely, differences between primary structural parameters of one kind, are used as external constraints of GED data analyses in order to obtain some experimental evidence for the conformational properties of a system of interest. So far the procedure has been applied successfully to the problems of 3-chlorobenzaldehyde,[1] 1,2-dimethylhydrazine,[2]

† Bevoegdverklaard Navorser, Belgian National Science Foundation (NFWO); on leave from Chemistry Department, University of Antwerp (U.I.A.), 2610 Wilrijk, Belgium.

(1) N. S. Chiu, J. D. Ewbank, M. Askari, and L. Schäfer, *J. Mol. Struct.*, **54**, 185-195 (1979).

0002-7863/82/1504-1476$01.25/0